Journal of the American Association for Laboratory Animal Science
Copyright 2011
by the American Association for Laboratory Animal Science

Vol 50, No 1
January 2011
Pages 61–64

Carbon Tube Electrodes for Electrocardiography-Gated Cardiac Multimodality Imaging in Mice

Philippe Choquet,[1] Christian Goetz,[1] Gaelle Aubertin,[1] Fabrice Hubele,[1] Sébastien Sannié,[2] and André Constantinesco[1,*]

This report describes a simple design of noninvasive carbon tube electrodes that facilitates electrocardiography (ECG) in mice during cardiac multimodality preclinical imaging. Both forepaws and the left hindpaw, covered by conductive gel, of mice were placed into the openings of small carbon tubes. Cardiac ECG-gated single-photon emission CT, X-ray CT, and MRI were tested (n = 60) in 20 mice. For all applications, electrodes were used in a warmed multimodality imaging cell. A heart rate of 563 ± 48 bpm was recorded from anesthetized mice regardless of the imaging technique used, with acquisition times ranging from 1 to 2 h.

Abbreviations: ECG, electrocardiography; SPECT, single-photon emission CT.

Molecular imaging techniques are mature tools for noninvasive diagnosis and follow-up of diseases in small rodents. However, mouse cardiac imaging remains a challenging task, needing gated acquisition triggered by the cardiac electrical activity of the subject.[14] The feasibility of ECG gated cardiac imaging in the living mouse has been demonstrated by using MRI, positron emission tomography, single-photon emission computed tomography (SPECT), and X-ray CT.[1,3,5-7,10,13,15,22,23] Cardiac multimodality imaging in mice has demonstrated accuracy for measuring wall tissue perfusion, heart mass, ejection fractions, ventricular volumes, stroke volume, and cardiac output under normal or pharmacologically stressed situations.[17] Nevertheless, repeated exams are needed for noninvasive longitudinal imaging studies of mice models of cardiac diseases or drug development characterization. Such examination would benefit from nontraumatic ECG electrodes that can be placed easily and quickly and yield a reliable signal. Moreover ECG-gated imaging exams are long-lasting procedures (for example, 1 to 2 h for dual SPECT–CT) and the skin–electrode electric contact is crucial for providing a reliable trigger throughout acquisition, given that evaluation of anesthetized mice implies the use of heated specific closed chambers. These imaging cells must include the ECG electrodes and corresponding leads in a limited space related to the small field of view of the cameras used. Finally the ECG electrode material should not contribute to image artifacts due to photon attenuation of gamma or X-rays or MR field and gradient interferences.[18,21]

In the literature, the optimal method for accurately and easily recording the ECG of mice remains poorly documented and appears specific to each research team. The most common approach uses 2-lead ECG, including subdermal needles, surface copper electrodes attached to the 2 front paws, and conventional and disposable human carbon fibers or pediatric and neonatal carbon electrodes or gold disk surface electrodes wrapped around the paws or attached to shaved forelimbs or chest of the mouse.[2,5,7,9,12,13,19] However, 2-electrode configurations used for triggering the acquisition of images generate low signal amplitude, and, because of the main direction of the ECG vector, 3 leads are recommended for better ECG quality, stability, and highest signal amplitude.[8,12,13]

Here we propose a new and simple design of ECG electrodes based on carbon tubes which we have adapted for multimodal imaging of small animals and for which set-up is easy and quick. We illustrate the practicality of our modified electrodes by using them in SPECT, CT, and MR imaging of mice.

Materials and Methods

Mice preparation and anesthesia. Adult mice (8 CD1, 4 nude, and 8 C57/Bl6; Janvier, le Genest-Saint-Isle, France) weighing 28 to 32 g were analyzed according to French regulations concerning small animal experimentation (authorization A 67-482-20). All mice were holoxenic animals housed 4 or 5 per cage in individually ventilated cages (Sealsale 1291H, Tecniplast France, Lyon, France). For all imaging procedures, mice were anesthetized with a gas mixture (1.5% to 2% isoflurane in air) and placed individually in a closed prewarmed multimodality imaging chamber (Minerve SA, Esternay, France; Figure 1).

Electrode design and set-up. ECG electrodes are made by cylindrical pultruded carbon tubes (length, 10 mm; inner diameter, 4.5 mm; outer diameter, 5.9 mm; Carbone-Composite Technology, Waldstetten, Germany; Figure 1). They are machined to fit the required design using model-building tools (Dremel 4000 3/34 kit, www.packardwoodworks.com). Ends of tubes were connected to the ECG module (Physiogard RSM784, Bruker/ODAM, Wissembourg, France) by using nonferrous and shielded coax leads. Both forepaws and the left hindpaw of a mouse were covered with conductive gel (ECG Cream, Schiller, Baar, Switzerland) and then inserted into the small carbon tubes (Figure 1). In all following imaging experiments except high-field MRI, the gating signal was sent directly to the corresponding imaging equipment.

SPECT–CT imaging experiment. Depending on the SPECT exam protocol, both intravenous and intraperitoneal routes were used in this study, but care was taken to keep the volume of intravenous tracer less than 0.2 mL to avoid significant changes in the total blood volume of mice. ^{99m}Tc-Tetrofosmin (Myoview, GE Healthcare, Chalfont, UK) or ^{201}Tl (CIS-Bio IBA, Paris, France) was used for myocardial wall perfusion, whereas

Received: 15 Apr 2010. Revision requested: 28 May 2010. Accepted: 07 Jul 2010.
[1]Department of Biophysics and Nuclear Medicine, Hôpitaux Universitaires de Strasbourg, Strasbourg, France, and [2]Minerve, Esternay, France.
[*]Corresponding author. Email: andre.constantinesco@chru-strasbourg.fr

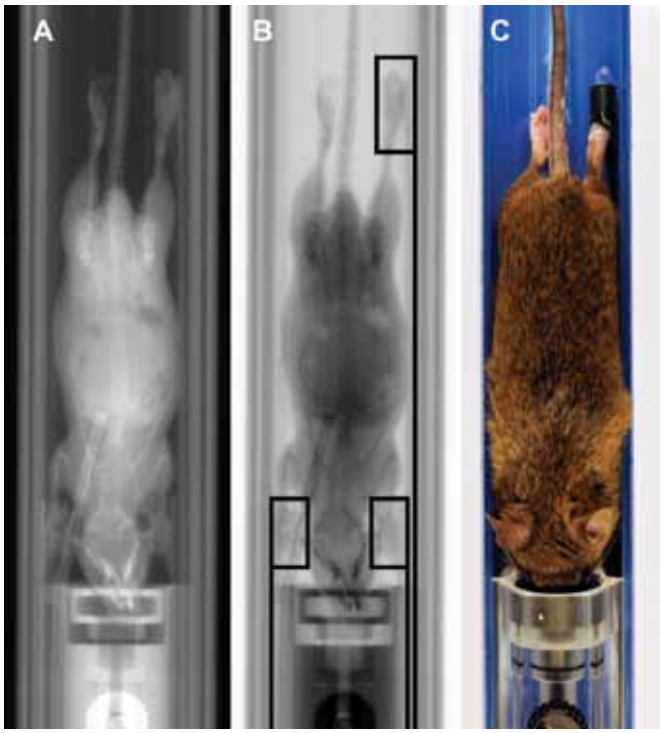

Figure 1. (A) CT 'scout' view of warmed-up imaging chamber used for preclinical multimodality imaging with ECG leads connected to carbon tube electrodes. (B) Schematic drawing of carbon-tube ECG electrodes, comprising tubes (length, 10 mm; inner diameter, 4.5 mm) and corresponding lead connections to the ECG module. (C) Close-up view of ECG carbon tube electrode surrounding mouse paw with conductive gel.

^{99m}Tc-human albumin (Vasculocis, CIS-Bio IBA) was used for blood pool imaging. Radiopharmaceuticals were administered 30 to 60 min before exam, with activities of 25MBq for ^{201}Tl and in the range of 500 to 750 MBq for ^{99m}Tc-Tetrofosmin and ^{99m}Tc-human albumin. For CT, a vascular long-lasting contrast agent (13.3 µL/g; FenestraVC, ART, Montreal, Canada) was injected intravenously or intraperitoneally 4 to 5 h before the exam. For SPECT–CT imaging, we used a fully integrated dual-modality imager (eXplore SPECZT Vision 120, GE Healthcare, Waukesha, WI). The SPECT apparatus is based on stationary solid-state cadmium zinc telluride pixellated detectors surrounding a rotating multipinhole (7 pinholes of 1-mm aperture) cylindrical collimator (axial and transverse fields of view of 80 and 32 mm, respectively). The CT equipment, combined back-to-back with the SPECT apparatus on the same axis, used a flat-panel detector combined with an X-ray rotating anode tube (80 kVP, 32 mA, and 16 ms exposure time).

The gated SPECT images acquisition protocol comprised a 360° helical acquisition protocol covering the mouse thorax with 15 s per projection, whereas the corresponding CT protocol involved a 'step and shoot' mode, with 220 projections covering 192° (Parker mode).

MRI experiment. A previously described dedicated low-field MR preclinical imaging system was used in this study.[4] Briefly, the vertical 0.1-T main magnetic field is generated by a water-cooled resistive magnet (Bouhnik SAS, Velizy–Villacoublay, France) with an 18-cm air gap. The encoding gradients have a maximal strength of 20 mT/m that can be reached in less than 0.5 ms. The radiofrequency solenoid coil (Figure 2) is tuned at 4.26 Mhz, which is the proton resonance frequency at 0.1 T. A

Figure 2. Warmed-up multimodality imaging chamber, with inserts showing radiofrequency coil around the mouse thorax for MRI and placement of mouse paw into carbon tube electrode with conductive gel.

3D gradient-echo ECG-gated T1-weighted fast low-angle shot (FLASH) imaging sequence with a flip angle of 60°, repetition time of 200 ms, echo time of 9 ms was used in this study.

A second experiment was designed to test our electrodes in a 2-forepaw configuration in a 11.7-T small-animal high-field MR imager (Bruker BioSpin, Karlsruhe, Germany) to assess the influence of gradient switching on the ECG signal. The main field was parallel to the body axis of the subject, and encoding gradients had a maximal strength of 150 mT/m which could be reached in 0.03 ms. Two-lead ECG then was recorded by using a small-animal dedicated module (SA Instruments, Stony Brook, NY).

Results

In all of the 60 in vivo imaging experiments tested in this study, the mean time necessary to place the 3 carbon tube electrodes on the 2 forepaws and left hindpaw of each mouse was less than 30 s.

ECG-gated SPECT–CT images and typical concurrent ECG recordings in mice. The CT numbers of the carbon tube electrodes were measured at 50 Hounsfield units and therefore had no influence on attenuation artifacts. The measured electrode impedance was 40 kΩ, which was far less than the input impedance of the signal conditioning unit (Physiogard RSM784, Bruker/ODAM).

Typical end-systole and end-diastole SPECT–CT images are presented in Figure 3. Isotropic spatial voxels of $0.9 \times 0.9 \times 0.9$ mm^3 and $0.1 \times 0.1 \times 0.1$ mm^3 were obtained for the SPECT and CT modes, respectively. An example ECG recording during image acquisition for each modality is included in Figure 3.

ECG-gated MR images and typical concurrent ECG recordings in mice. Figure 4 illustrates a midthoracic axial slice in end-systole and end-diastole with an in-plane pixel resolution of 0.5×0.5 mm^2 and a slice thickness of 1.7 mm. Also displayed is the ECG recorded with and without the imaging gradients, showing that gradient switching had no effect on ECG recording. In that case orientation of the gradients is perpendicular to the main axis of the carbon tube electrode. In Figure 5, we show that switching gradients mimicking a gradient echo-imaging sequence in a high-field MRI small-animal system (main magnetic field of 11.7 T parallel to the mouse body's axis and 2-forepaw carbon tube electrode configuration) had little influence on the

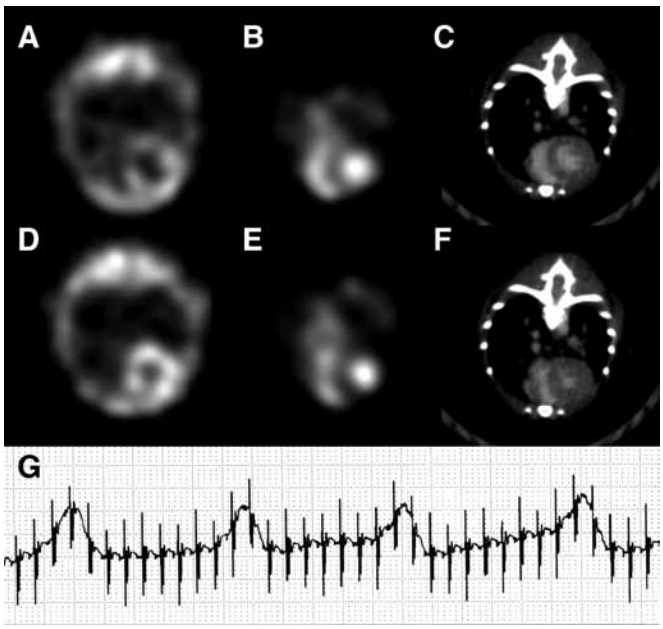

Figure 3. Example of mouse ECG-gated SPECT–CT midthoracic axial slice images with cubic voxels of $0.9 \times 0.9 \times 0.9$ mm^3 and $0.1 \times 0.1 \times 0.1$ mm^3, respectively. Myocardial left ventricle perfusion ^{201}Tl SPECT at (A) end-diastole and (D) end-systole. Blood-pool ^{99m}Tc SPECT of both ventricles in (B) end-diastole and (E) end-systole. Contrast CT midventricular slices in (C) end-diastole and (F) end-systole. (G) Typical ECG recording during SPECT–CT image acquisition.

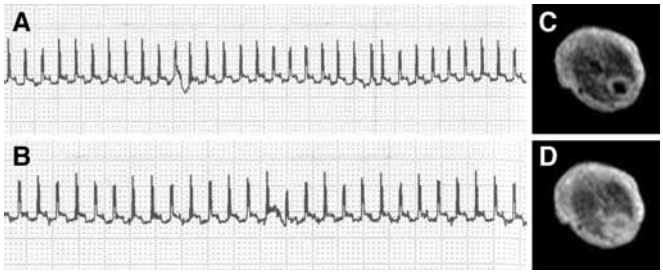

Figure 4. Mouse ECG recordings inside a 0.1-T magnetic field (A) without and (B) with imaging gradients, showing no influence of gradient switching. (C) End-diastole and (D) end-systole MRI midthoracic axial slices, with an in-plane pixel size of 0.5×0.5 mm^2 and slice thickness of 1.7 mm.

recorded ECG. The R wave is clearly visible and can be used for image-triggering purposes despite an increased noise level superimposed on the ECG signal of the mouse.

Mean value and variation of heart rate recorded during imaging experiments. Heart rate measured was 563 ± 48 bpm for all imaging experiments (n = 60) in the 20 mice examined in this study. Because preclinical cardiac imaging sessions tend to be lengthy procedures, we tested the variation of the heart rate during the SPECT–CT imaging procedure used in this study. Figure 6 illustrates the corresponding heart rate evolution and histogram recorded during a typical data acquisition session.

Discussion

In micro CT, SPECT, positron emission tomography, and MRI, multiple heart cycles must be recorded to acquire consecutive time bins over the RR cycle in order to freeze cardiac motion. In that respect, obtaining a strong and stable ECG signal for triggering image acquisition is extremely important.[9,12] To achieve this goal noninvasively, 3-lead bipolar surface ECG protocols are desirable to provide a maximal signal (lead II or

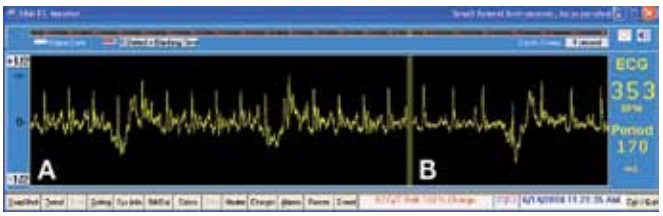

Figure 5. Mouse ECG recordings inside a 11.7-T magnetic field (A) with and (B) without imaging gradients, showing increased noise during gradient switching but good R wave detectability.

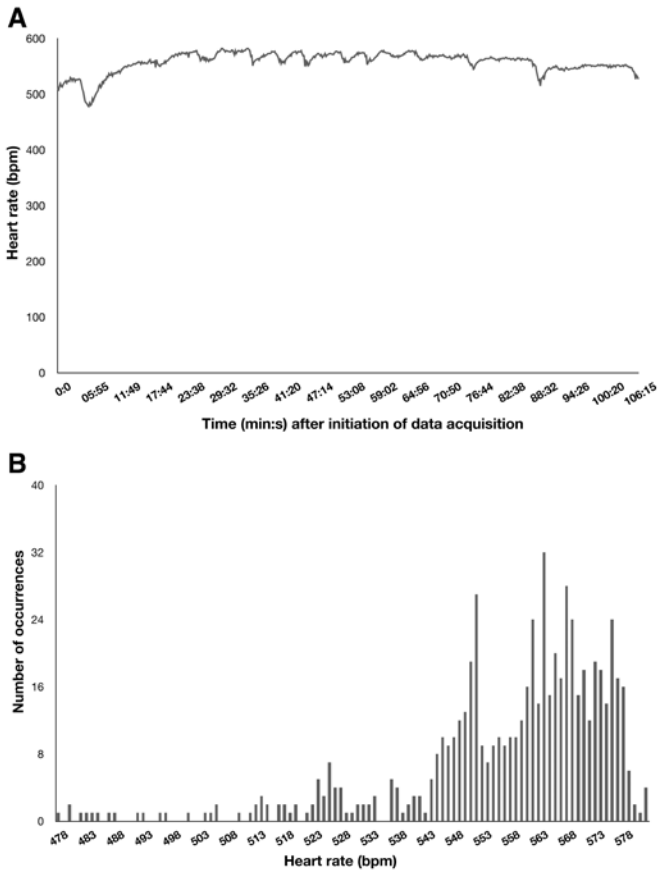

Figure 6. Example of (A) time evolution and (B) corresponding histogram of heart rate in a mouse during typical ECG-gated SPECT–CT image acquisition using the described carbon tube electrodes.

III).[20] Moreover, subdermal needles or firmly wrapping pediatric electrodes[9] after shaving the chest or around the paws of animals to strengthen the signal is a time-consuming task that could cause discomfort and pain. The cylindrical design of the proposed carbon tube electrodes overcame these limitations, and the mean heart rate we measured was similar to that of unanesthetized mice.[20] For the safety and comfort of the subject as well as quality of the acquired images, closed multimodal imaging chambers able to maintain anesthetized mice at a controlled temperature during imaging procedures are now common in state of the art systems. However, the small field of view of the imaging systems dedicated to mice restricts the space available for positioning of the ECG electrodes in the imaging chamber. In that respect, the design of the carbon tube electrode is particularly beneficial given the limited space available in the imaging chambers used in preclinical imaging.

The carbon material of the proposed electrodes is particularly appropriate for CT and SPECT and caused no image degrada-

tion in MRI.[19] However, in small-animal MRI and in the present electrode and lead configuration, there are 2 kinds of current loops that can induce voltage artifacts into the ECG signal. The first is composed of 2 of the 3 cables, the mouse tissue between the electrodes related to those cables, and the input impedance of the ECG preamplifier.[21] In the specific case of low-field MRI magnets delivering a main magnetic field perpendicular to the main axis of the animal's body, as in our 0.1-T imager, we demonstrated that the recorded ECG signal contains no induced voltage. In the case of small-animal high-field MRI magnets when field lines are parallel to the body of the animal, keeping the plane of each loop parallel to the time-variable magnetic field lines greatly minimizes the induced artifacts.[21] Only in high-field MRI systems is there a second current loop, corresponding here to the cylindrical design of the carbon tube itself, which acts as a small conductive loop that is perpendicular to the changing field lines. However, the induced voltage is greatly reduced according to the Faraday and Ohm laws due to the small radius and low impedance of the carbon tube.[19,21] In the same way, eddy currents are reduced in the proposed design due to the value of the measured carbon electrode impedance.[19] The use of carbon instead of copper caused no image degradation,[19] and we observed in our high-field MRI experiment that few induced artifacts were generated in the recorded ECG even when only 2 forepaw carbon tube electrodes were used.

Most of the constraints to obtaining a reliable ECG signal for triggering multimodal preclinical imaging systems were eliminated by the simple design of the proposed small carbon tube electrodes, for which set-up was noninvasive, easy, and quick. We used our electrode set-up in different strains because various features of the mouse ECG (for example, amplitude of the QRS complex) are under partial genetic control.[11] We obtained a reliable ECG trigger in all of the tests we performed. Practical application of our carbon tube electrodes was demonstrated in different preclinical imaging modalities including SPECT, CT, and MRI but might easily be extended to positron emission tomography and echography. Moreover, because multimodality preclinical imaging techniques in mice are now widely accepted methods for longitudinal evaluation of disease progression and follow-up of pharmacologic interventions, continuous concurrent ECG is recommended to confirm the cardiovascular status of the animal during all imaging protocols.[16] In that respect, the use of the carbon tube electrodes proposed here likely will greatly facilitate not only ECG recording in mice for triggering image acquisition but also for ECG signal analysis and survey of cardiac status during the long acquisition time of multimodal imaging procedures. In our experience, we have never lost the ECG signal regardless of the imaging technique and acquisition time used. Finally the same electrode design but with a larger diameter potentially could be applied for rats.

Here we developed noninvasive carbon tube electrodes to facilitate ECG recording in mice for cardiac multimodality preclinical imaging. Carbon tubes were fit by using conductive gel to both forepaws and the left hindpaw of mice for 3-lead ECG recording. ECG-gated multimodality imaging techniques including SPECT, CT, and MRI were tested successfully.

Acknowledgment

We are grateful to General Electric Healthcare for their constant help and support.

References

1. **Badea CT, Fubara B, Heflund L, Johnson G.** 2005. 4D microCT of the mouse heart. Mol Imaging **4:**110–116.
2. **Berr S, Roy R, French B, Yang Z, Gilason W, Kramer C, Epstein F.** 2005. Black blood gradient echo cine magnetic resonance imaging of the mouse heart. Magn Reson Med **53:**1074–1079.
3. **Chin BB, Metzler S, Lemaire A, Curcio A, Vemulapalli S, Greer K, Petry N, Turkington T, Colemen R, Rockman H, Jaszczak R.** 2007. Left ventricular functional assessment in mice: feasibility of high spatial and temporal resolution ECG-gated blood pool SPECT. Radiology **245:**440–448.
4. **Choquet P, Breton E, Goetz C, Constantinesco A.** 2009. Dedicated low-field MRI in mice. Phys Med Biol **54:**5287–5299.
5. **Constantinesco A, Choquet P, Monassier L, Israel-Jost V, Mertz L.** 2005. Assessment of left ventricular perfusion, volumes, and motion in mice using pinhole-gated SPECT. J Nucl Med **46:**1005–1011.
6. **Croteau E, Bénard F, Cadorette J, Gauthier ME, Aliaga A, Bentourkia M, Lecomte R.** 2003. Quantitative gated PET for the assessment of left ventricular function in small animals. J Nucl Med **44:**1655–1661.
7. **Feintuch A, Zhu Y, Bishop J, Davidson L, Dazai J, Brineau B, Hankelman R.** 2007. 4D cardiac MRI in mouse. NMR Biomed **20:**360–365.
8. **Franco F, Dubois S, Peschock R, Shohet R.** 1998. Magnetic resonance imaging accurately estimates LV mass in a transgenic mouse model of cardiac hypertrophy. Am J Physiol **274:**H679–H683.
9. **Gilson WD, Kraitchman D.** 2007. Cardiac magnetic resonance imaging in small rodents using clinical 1.5 T and 3.0 T scanners. Methods **43:**35–45.
10. **Goetz C, Monassier L, Choquet P, Constantinesco A.** 2008. Assessment of right and left ventricular function in healthy mice by blood pool pinhole gated SPECT. C R Biol **331:**637–647.
11. **Goldbarg A, Hellerstein H, Bruell J, Daroczy A.** 1968. Electrocardiogram of the normal mouse, *Mus Musculus*: general considerations and genetics aspects. Cardiovasc Res **2:**93–99.
12. **Hoyt R, Hawkins J, St Claire M, Kennett M.** 2006. Mouse physiology, p 25–78. In Fox J, Berthold S, Davisson M, Newcomer C, Quimby F, Smith A, editors. The mouse in biomedical research, 2nd ed, vol 3. New York (NY): Elsevier
13. **Kreissl MC, Wu H, Stout D, Ladno W, Schindler T, Zhang X, Prior J, Prins M, Chatziioannou A, Huang S, Schelbert H.** 2006. Noninvasive measurement of cardiovascular function in mice with high-temporal-resolution small-animal PET. J Nucl Med **47:**974–980.
14. **Lahoutte T.** 2007. Monitoring left ventricular function in small animals. J Nucl Cardiol **14:**371–379.
15. **Nahrendorf M, Badea C, Hedlund L, Figueiredo J, Sosnovik D, Johnson G, Weissleder R.** 2007. High-resolution imaging of murine myocardial infarction with delayed-enhancement cine microCT. Am J Physiol Heart Circ Physiol **292:**H3172–H3178.
16. **Nicholson A, Klaunberg B.** 2008. Anesthetic considerations for in vivo imaging studies, p 629–637. In: Fish R, Danneman P, Brown M, Karas A, editors. Anesthesia and analgesia in laboratory animals, 2nd ed. New York (NY): Elsevier
17. **Tsui BM, Kraitchman D.** 2009. Recent advances in small animal cardiovascular imaging. J Nucl Med **50:**667–670.
18. **Vallee JP, Ivancevic M, Nguyen D, Morel D, Jaconi M.** 2004. Current status of cardiac MRI in small animal. MAGMA **17:**149–156.
19. **Van Gederingen HR, Sprenger M, de Ridder J, Van Rossum A.** 1989. Carbon-fiber electrodes and leads for electrocardiography during MR imaging. Radiology **171:**872.
20. **Wehrens XH, Kirchoff S, Doevendans P.** 2000. Mouse electrocardiography: an interval of 30 years. Cardiovasc Res **45:**231–237.
21. **Wendt RE 3rd, Rokey R, Vick W, Johnston D.** 1988. Electrocardiographic gating and monitoring in NMR imaging. Magn Reson Imaging **6:**89–95.
22. **Wiesmann F, Ruff J, Hiller K, Rommel E, Haase A, Neubauer S.** 2000. Developmental changes of cardiac function and mass assessed with MRI in neonatal, juvenile, and adult mice. Am J Physiol Heart Circ Physiol **278:**H652–H657.
23. **Wu M, Tang R, Gao D, Ido A, O'Connell J, Hasegawa B.** 2000. ECG-gated pinhole SPECT in mice with millimeter spatial resolution. IEEE Trans Nucl Sci **47:**1218–1221.